

N 69 22195  
NASA CR 100577

**CASE FILE  
COPY**

FINAL REPORT ON COMPUTER EXPERIMENTS IN PLASMA PHYSICS

Study of Transport Properties and Distribution Function

Dynamics in One Dimensional Plasma Models

NASA Grant NGR 44-001-050

## One Dimensional Study of Tonks-Daltnner Resonances

S. Ramchandran and M. Eisner

The resonances occurring in a cylindrical plasma column being driven by a transverse electric field have been the subject of much investigation since they were initially observed by Tonks.<sup>(1,2)</sup> Although only a single resonance at the plasma frequency was expected on the basis of simple theories, in fact a series of resonances were observed. Tonks attributed these to the inhomogeneity of the plasma density. Crawford<sup>(3)</sup> showed that these are two types of modes which propagate radially in a non-uniform cylindrical plasma column, the first mode is similar to that which would exist in a cold plasma while the second depends on the electron temperature. Leavens<sup>(4)</sup> solved the Vlasov equation to obtain the resonance spectrum of a realistic model of a plasma cylinder including a sheath. He reduced the cylinder to a thin one dimensional slab of collisionless thermal plasma. He found that there was no relation between the first resonance frequency and the average plasma resonance and also found resonances above the series limit.

The present work uses a plasma similar to that used by Leavens but the analysis is based on a sheet plasma dynamics rather than solutions of the conductivity kernel as used by Leavens. The sheet model has been extensively used and the work of Dawson<sup>(5)</sup> and Elridge and Feix<sup>(6)</sup> are useful guides for the detailed procedures.

## Description of the Computer Experiment

In setting up the numerical experiment, a one-dimensional two-component plasma is used. Electrons are distributed according to the Maxwellian velocity distribution. Heavy ions are kept stationary and distributed so as to satisfy the Poisson equation. The distribution function for the electrons, used is

$$f(x, v) = n_0 \left( \frac{m}{2\pi kT} \right)^{1/2} e^{-e\phi(x)/kT} e^{-1/2 m v^2 / kT}$$

where  $n_0$  is a constant,  $m$  is the mass of the electron,  $\phi(x)$  is the potential which is a function of position  $x$ ,  $v$  is the velocity and  $kT$  is the thermal energy.

It is assumed that the mass  $m$  of the electron is equal to 1 and the mass of ion is very large. Electron has a charge  $e_- = -1$  and the charge of ion is  $e_+ = +1$ .

The total thickness of the system is 284.19 arbitrary units of length and is divided into 60 equal space intervals, each of length 4.7365 units. The first 52 of these intervals are in the plasma and the remaining 8 are in the sheath. The electric field  $E_0$  in the plasma is constant and increases linearly in the sheath (Refer Figure 3). The fields are measured in units of  $kT/1/2 \lambda_D^0$  where  $kT$  is the thermal energy, and  $\lambda_D^0$  is the Debye length evaluated at the position  $X=0$ . The constant field  $E_0$  in the plasma has a value 0.01625. The

plasma frequency at the sheath edge,  $\omega_p(s)$  has a value of 0.1344 after scaling it to the plasma frequency at the position  $X=0$ .

For the generation of plasma in the numerical experiment the following procedure was used. First the total length of the system was divided into small segments of  $\frac{1}{4}$  of the space interval mentioned above. Then the distribution function  $f(x,v)$  was integrated over  $x$  and  $v$  between the proper limits to obtain the corresponding number of particles in each segment. The electrons and the ions are arranged alternately, the electrons at equal spatial intervals and ions at random intervals. The initial electron velocities are obtained according to the Maxwellian velocity distribution by using a random number generator subroutine.

A total of 19,014 particles are used in the system, including electrons and ions out of which 18,862 are in the plasma, the rest in the sheath.

The electrons are emitted from the wall at the position  $X=0$ , with a Maxwellian velocity distribution. The inner wall at the position  $X=0$  also absorbs all the electrons which strike it. A few of the electrons reach the floating wall at the position  $X=L$ , where  $L$  is the length of the system.

Oscillating electric fields with various frequencies and amplitudes are applied to this system and the dynamics of the system are observed at intervals

of time  $\Delta T$ . The quantities of interests measured are the potential energy, kinetic energy, the total energy and the current which are defined as follows:

$$\text{Potential energy} = \sum_{\lambda=1}^N [E(\lambda+1)]^2 (\chi_{\lambda+1} - \chi_{\lambda})$$

$$\text{Kinetic energy} = \frac{1}{2} \sum_{\lambda=1}^N v_{\lambda}^2$$

Total energy = Kinetic energy + Potential energy

$$\text{Current} = \frac{1}{N} \sum_{\lambda=1}^N v_{\lambda}$$

Here, N is the total number of particles in the system. The results are then

Fourieranalyzed using the equation

$$F(\omega) = \frac{1}{2\pi} \int_{-\infty}^{\infty} F(t) e^{-i\omega t} dt$$

The plasma model was set up and the numerical experiments were conducted on the UNIVAC 1108 electronic computer at the National Aeronautics and Space Administration at Houston.

During the experiment, the current and energy were measured at intervals of 0.01 of an electron plasma period. The system was subjected to the oscillating electric field for about 1.5 plasma periods. The time taken to generate the plasma initially, was approximately 2 minutes on UNIVAC 1108 computer. On the average, it took about 25 minutes of computer time for 20 individual measurements. The results are then Fourier analyzed to find the frequency dependence.

## Results and Discussion

The numerical experiment was done for several different frequencies of the impinging oscillating electric field. Also two different amplitudes were used for the driving field and the driving field consists of square waves.

The results of the numerical experiments are presented graphically (Figures 4-17) showing the relationship of frequencies used in the study to the values of current obtained in the analysis. In the results shown, Figures 4 through 11, the amplitude of the driving field used was 1.0 whereas in Figures 12 through 17, the amplitude used was 0.1. The frequencies are expressed in terms of the plasma frequency at  $X = 0$  in the plasma model and the current is expressed in arbitrary units. Figures 4 through 7 shows the relationship of the frequencies used to the absolute value of the current whereas Figures 8 through 11 are the corresponding real and imaginary parts of the current.

Specifically, Figure 4 gives the dependence of current on frequency when the driving electric field is a square wave of period  $T = 0.30$  ( $\frac{\omega}{\omega_{pe}} = 0.21$ ). Here the first resonance occurs at the frequency 0.13 and the sharpest resonance is seen at the frequency 0.19. There are also about 5 weaker resonances occurring at frequencies 0.26, 0.31, 0.35, 0.51 and 0.55. In Figure 5 is shown the relationship, of current versus frequency for a driving field of period 0.35

(  $\frac{\omega}{\omega_{pc}}$  = 0.18). Here also, as shown in Figure 4, the first resonance is at the frequency 0.13 and the sharpest resonance is at the frequency 0.19. There are additional weaker resonances, occurring at the frequencies 0.25, 0.31, 0.35, 0.45, 0.51, and 0.56. In the case of driving field of period 0.40 (  $\frac{\omega}{\omega_{pc}}$  = 0.15), the situation is slightly different (Figure 6). The first and the sharpest resonance is at the frequency 0.14 and all the other resonances are weak, the second resonance being at the frequency 0.20. There are at least 6 more weaker resonances, the frequencies being at 0.25, 0.30, 0.35, 0.40, 0.46, 0.52. In Figure 7, the driving field has a period 0.48 (  $\frac{\omega}{\omega_{pc}}$  = 0.13). This is very similar to that of Figure 6, the first and sharpest resonance being at the frequency 0.14 and the second resonance being at the frequency 0.20. Here also except the first one, the rest of the resonances are weak and occurs at frequencies 0.24, 0.30, 0.34, 0.41 and 0.46. The next set of results are for the driving fields of amplitude 0.1. In Figure 12, is shown the relationship of frequency versus current for a driving field of period 0.30. Here the first resonance occurs at the frequency 0.13 and the second, the sharpest resonance occurs at the frequency 0.19 and there are additional, several weaker resonances occurring at frequencies 0.26, 0.30, 0.35, 0.40, 0.45, 0.50 and 0.56. Figures 13 and 14 are the frequency dependence on current for the driving fields with

periods 0.33 ( $\frac{\omega}{\omega_p(s)} = 0.19$ ) and 0.35 ( $\frac{\omega}{\omega_p(s)} = 0.18$ ) respectively. In both these cases the first resonance occurs at the frequency 0.13 and the second is the sharpest resonance and occurs at the frequency 0.19. In Figure 13, the additional 7 weaker resonances occurs at frequencies 0.25, 0.30, 0.35, 0.40, 0.45, 0.50 and 0.56. In Figure 14, the additional weaker resonances are seen at frequencies 0.25, 0.30, 0.34, 0.40, 0.45, 0.50 and 0.56.

All these results clearly emphasizes the fact that there is no relationship between the first resonance frequency and the average plasma frequency, as predicted by Dattner's experimental investigation <sup>(7)</sup> and the present result agrees with the results of Leavens. <sup>(8)</sup> An absolute comparison with any of the earlier investigations is not possible in this case, since we have used a weaker sheath in the numerical experiment. It has been shown <sup>(8)</sup> that it is the sheath which influences the position of the resonances. For a stronger sheath, there is no resonance below the plasma frequency at the sheath edge ( $\omega_p(s)$ ). This cut-off at  $\omega_p(s)$  is not seen in this experiment. Hence, it can be said that a weaker sheath really would behave differently and is possible to bring resonances below  $\omega_p(s)$ . In the present investigation the number of resonances observed is also more as compared to the case of a stronger sheath used by Leavens. <sup>(4)</sup> It is also interesting to note that the first resonance



frequency increases with a smaller driving field frequency. For a stronger driving field, (amplitude = 1.0) the higher resonances are not as well defined as in the case of a weaker driving field (amplitude = 0.1). This is probably due to the effect of non-linear processes in the case of stronger driving fields. This effect on higher resonances is significantly noticeable in the case of higher driving field frequencies.

## Conclusions

The purpose of this work was to investigate the resonances in a one-dimensional, two component, non-uniform sheath-bounded plasma. A one-dimensional plasma with appropriate boundary conditions was simulated. The system was driven by oscillating electric fields of various frequencies and the corresponding time varying currents were obtained. The time varying current was then Fourier analyzed to obtain the frequency dependence. The numerical experiment was performed for two different amplitudes. This one-dimensional charge sheet model is a simple and sensible model system, exhibiting some of the properties of a plasma. Several of the theoretical predictions have been verified using one-dimensional homogeneous plasma. The present experiment proves its applicability to non-homogeneous one-dimensional system.

It was found that the model did show resonances. Although it was not possible to make an absolute comparison with the results obtained by earlier investigators, because of the difference in the sheath strength, the following conclusions could be made.

- (1) There is no relation between the first resonance frequency and the average plasma frequency, in agreement with the result obtained by Leavens.

- (2) The sheath strength influences the resonances, and a weaker sheath would show resonances below  $\omega_p(s)$ , whereas a stronger sheath would cut off the resonances at  $\omega_p(s)$ . This weaker sheath also increases the number of resonances.
- (3) There is a shift in the first resonance frequency as the frequency of the driving field changes, in the case of a weaker sheath.
- (4) In the case of stronger driving fields, the effect of non-linear processes is seen for higher resonances.

It would be interesting to do the experiment with various sheath strengths, as the plasma behave differently for a weaker sheath.

#### References

1. L. Tonks, Phys. Rev. 37, 1458 (1931a).
2. L. Tonks, Phys. Rev. 38, 1219 (1931b).
3. F. W. Carwford, Microwave Laboratory Report No. 1945
4. W. M. Keavens, Dissertation, University of California, San Diego, California.
5. J. Dawson, Phys. Fluids, 5, 445 (1962).
6. O. C. Eldrige and M. Feix, Phys Fluids, 6, 398 (1963).

Case - 1 - Period - 0.30

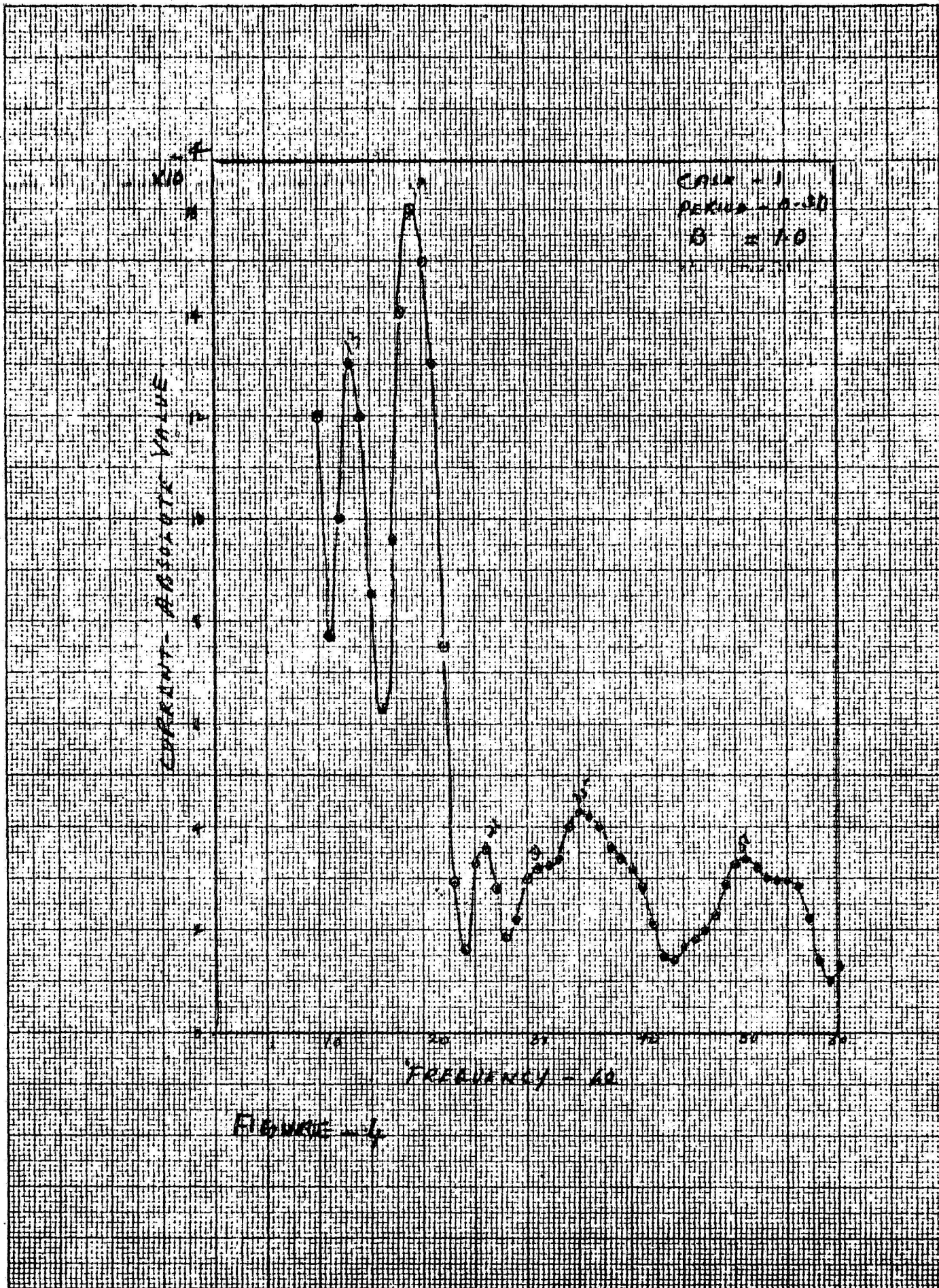


Figure - 1

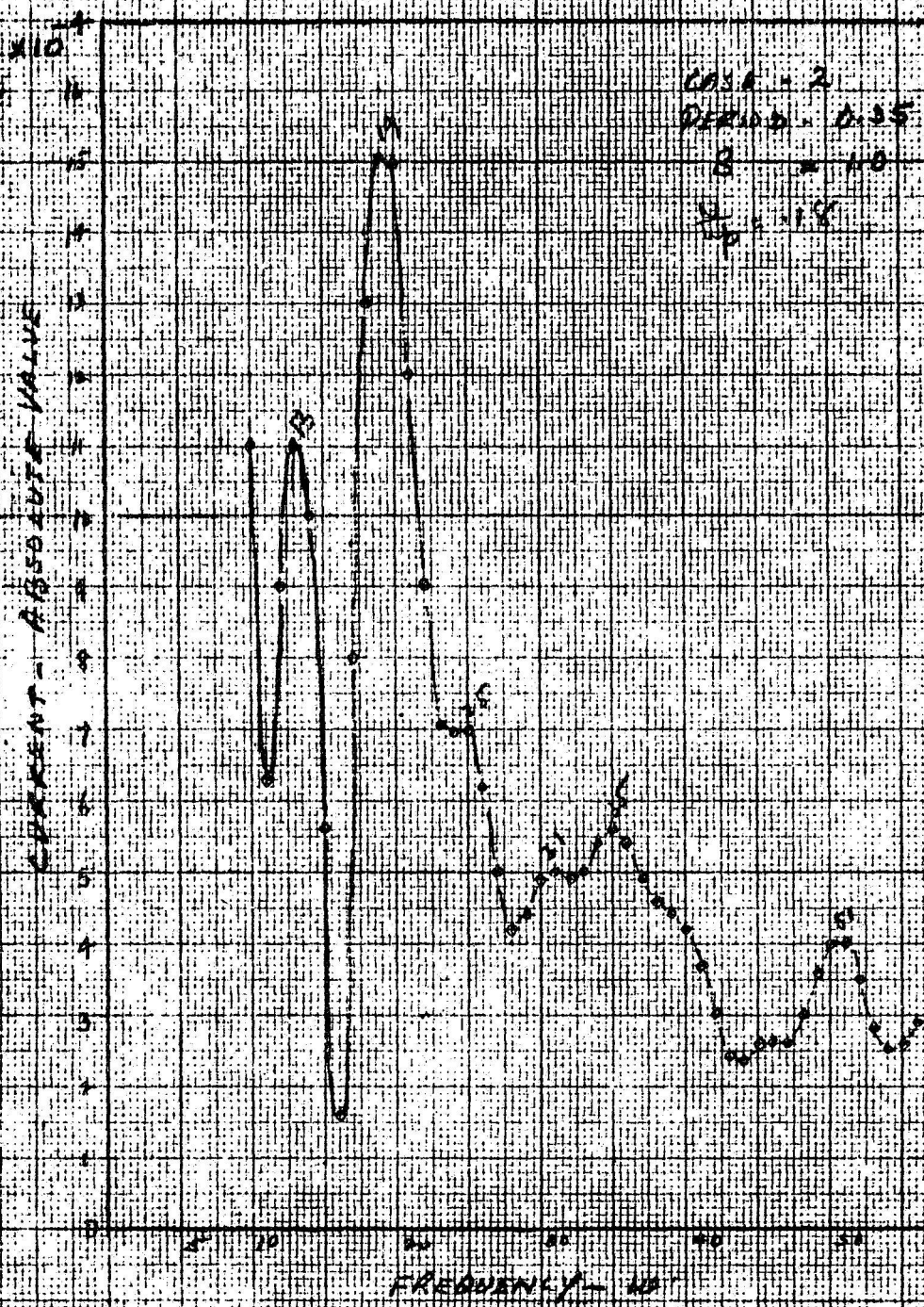


FIGURE - 5

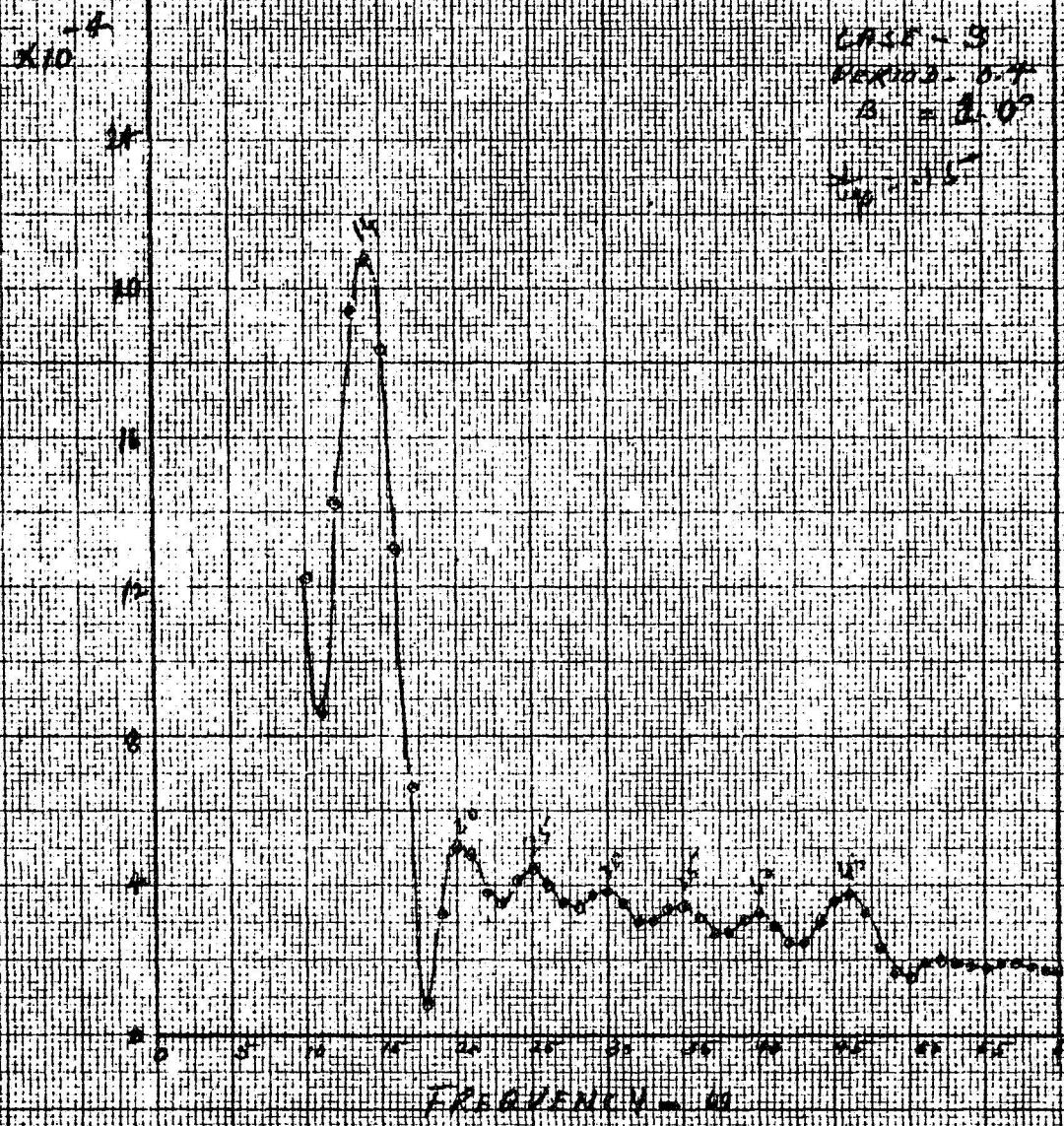


FIGURE - 5

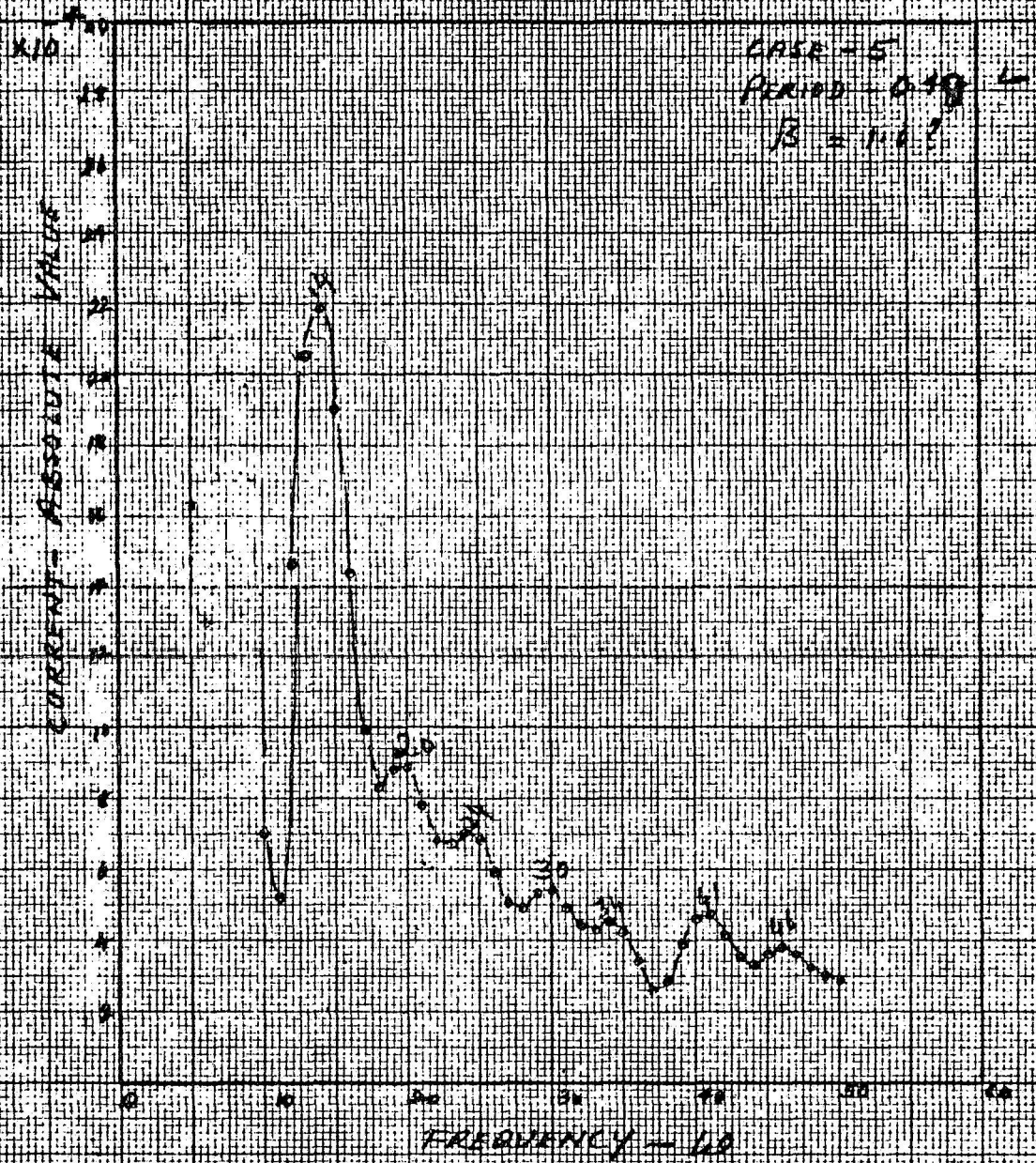


FIGURE - 7

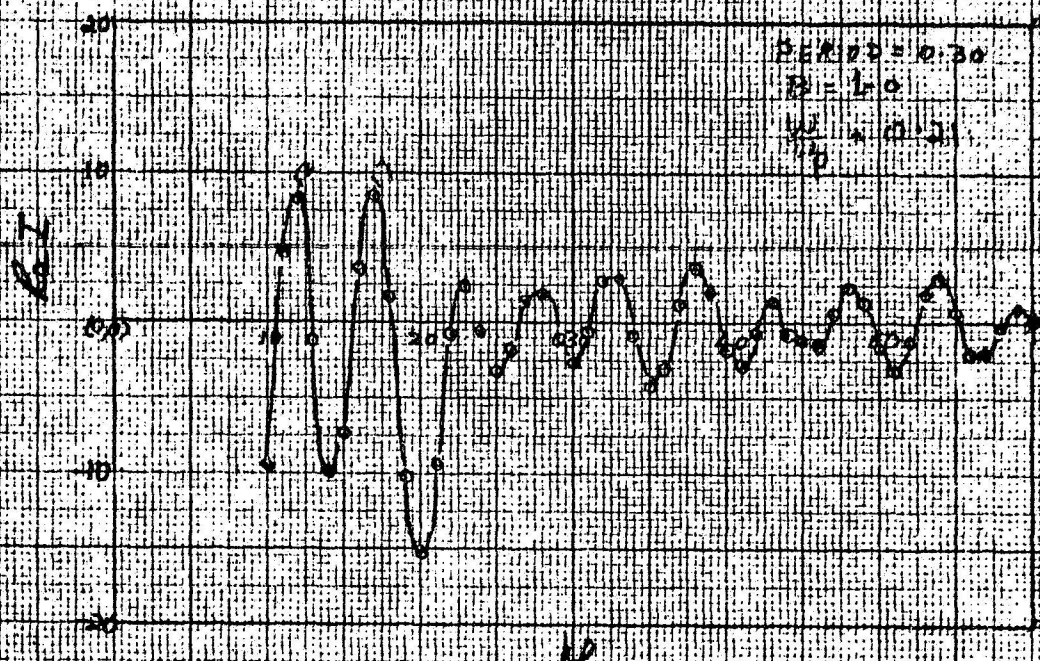


FIGURE 4



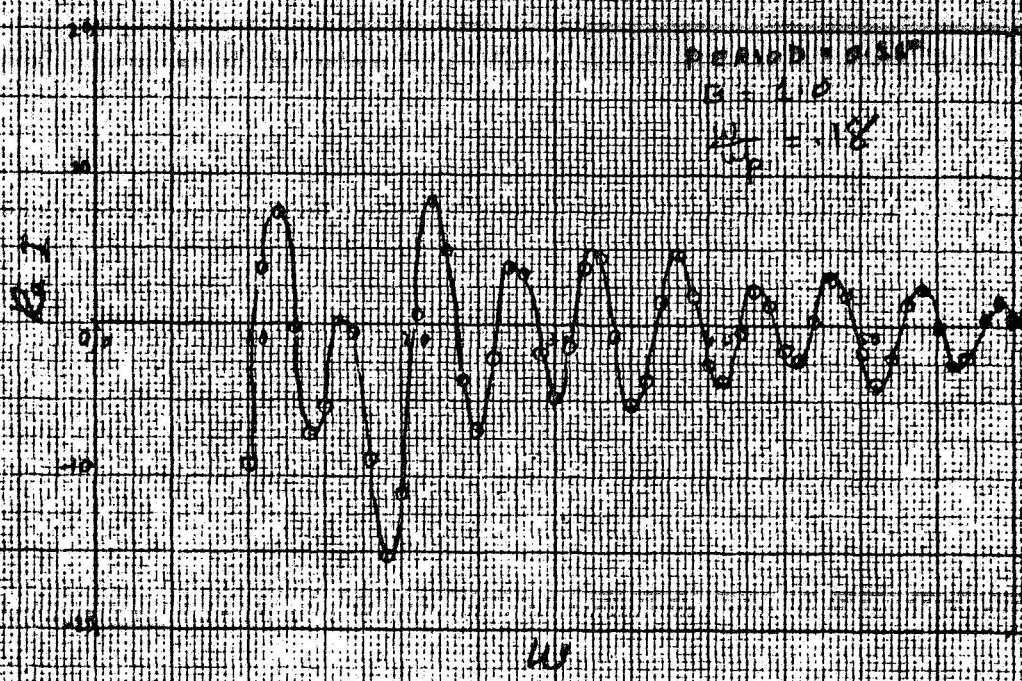


FIGURE - 9

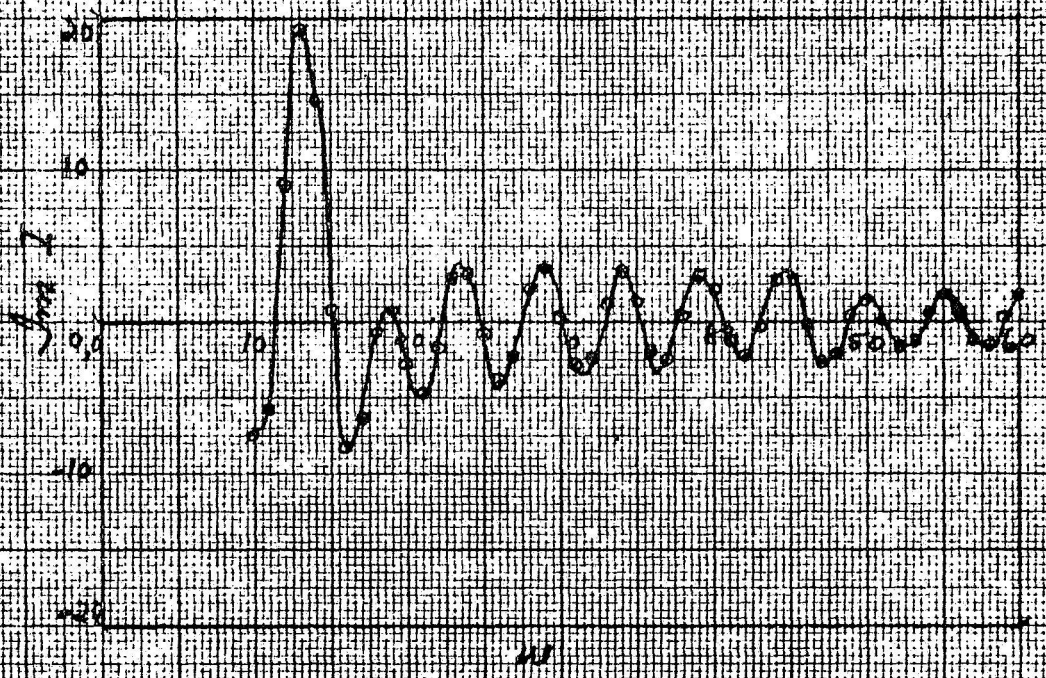
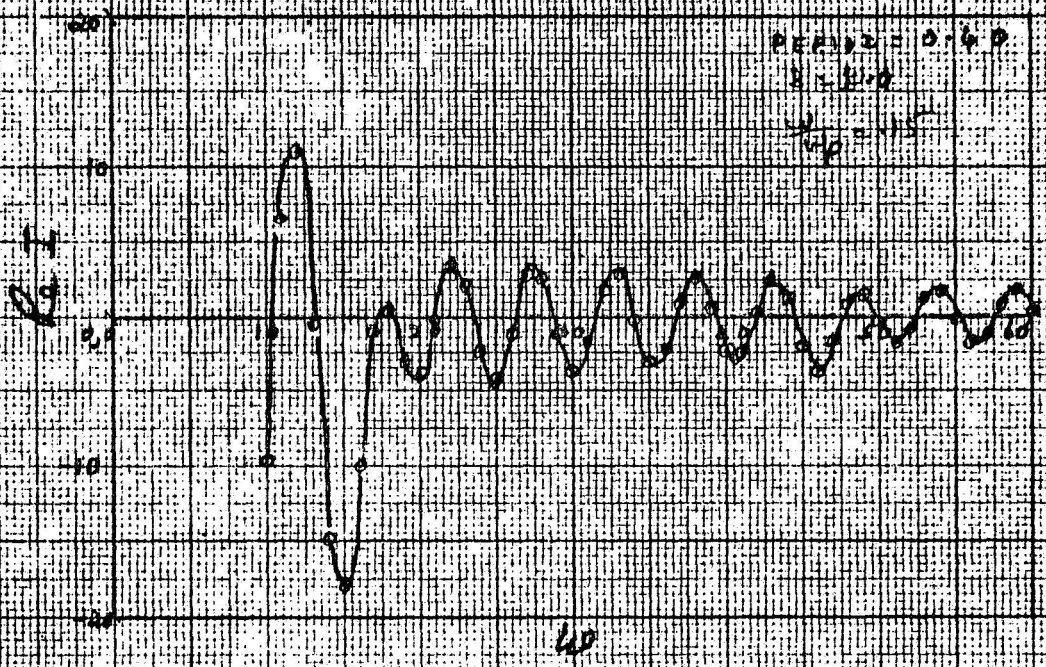


FIGURE 10

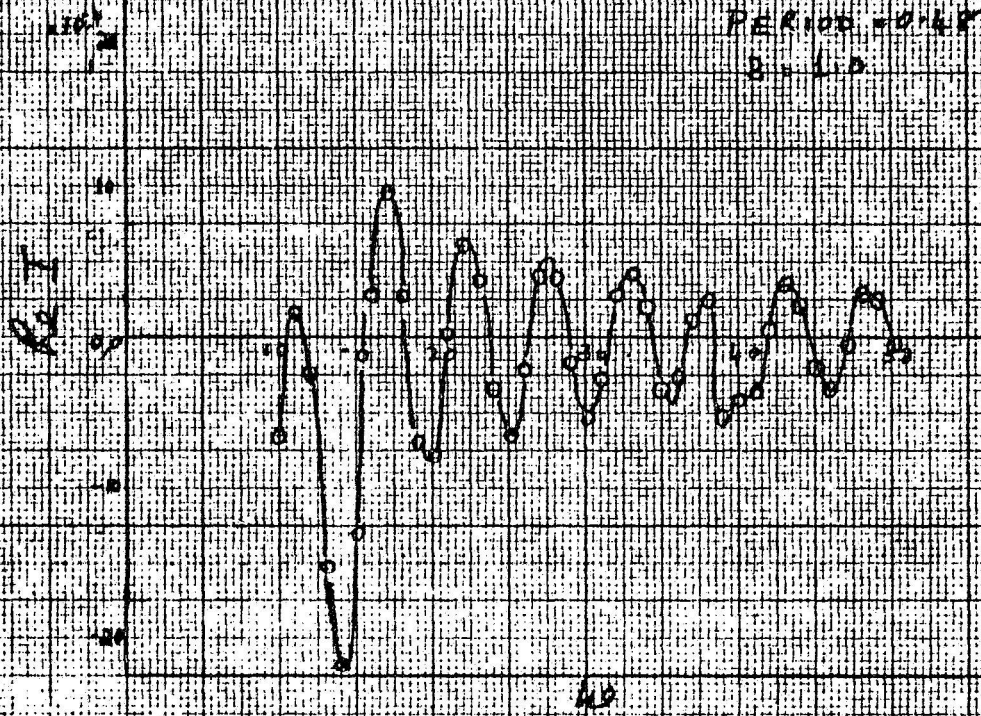


FIGURE 12

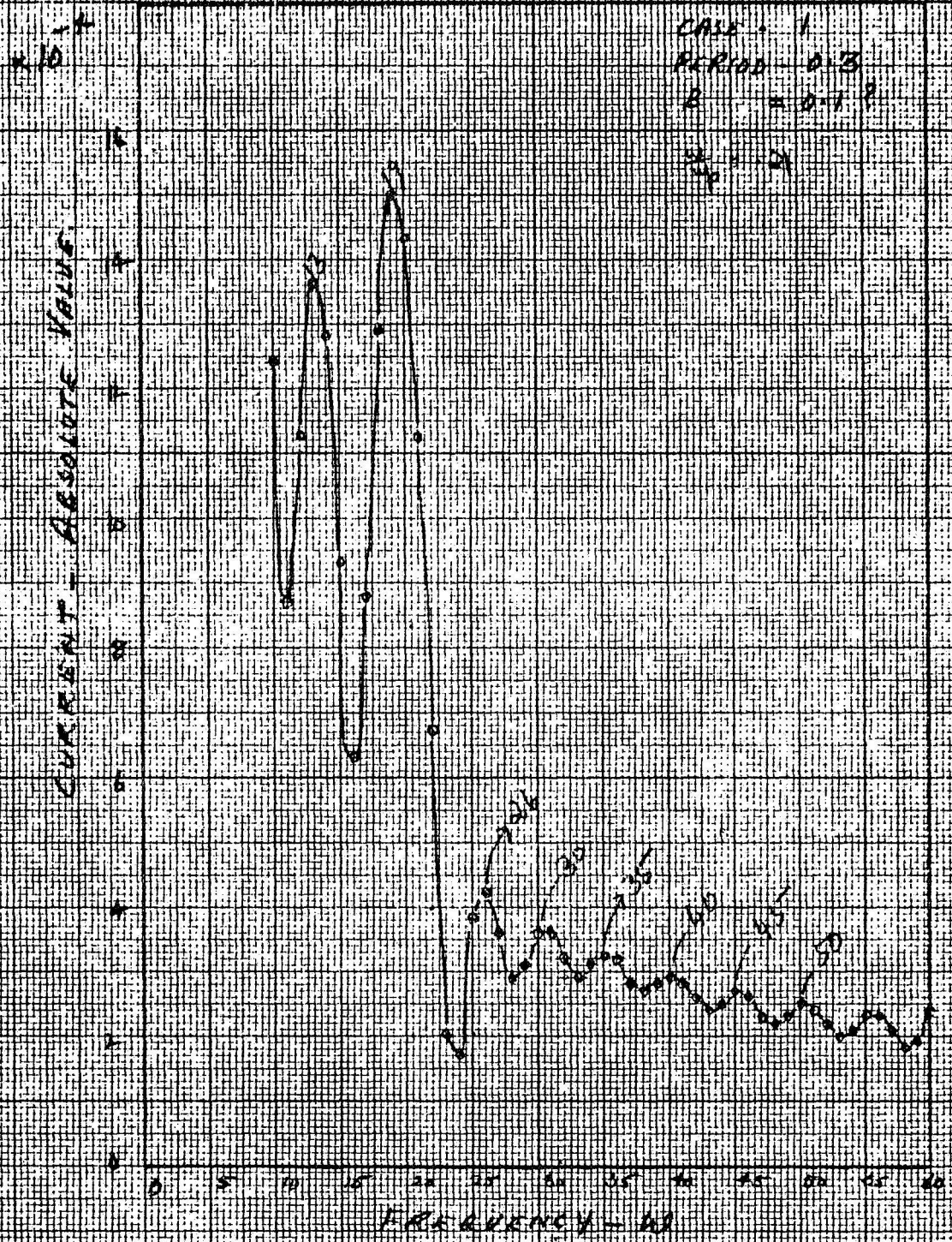


FIGURE-12

MADE IN U. S. A.

MILLIMETER

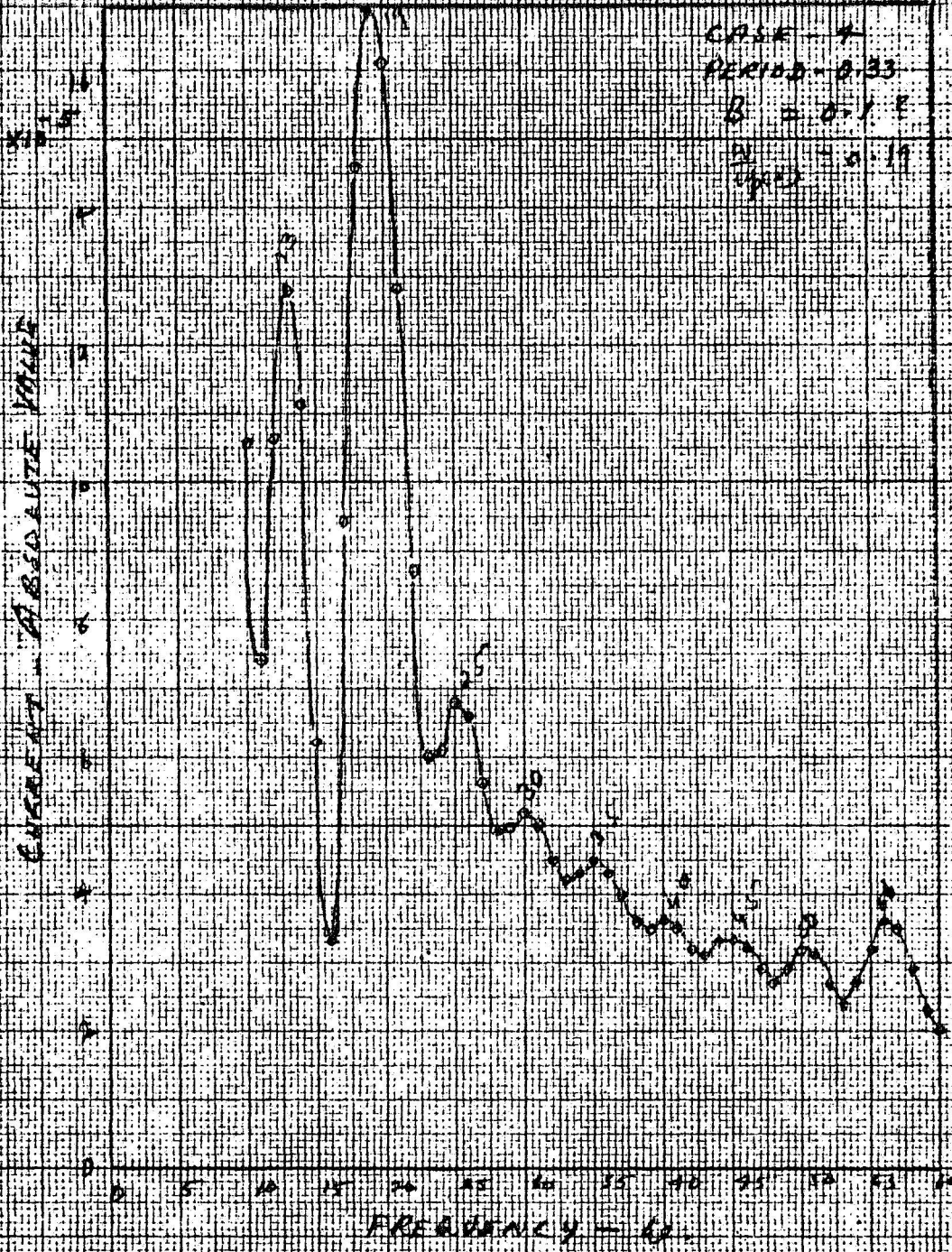


FIGURE 13

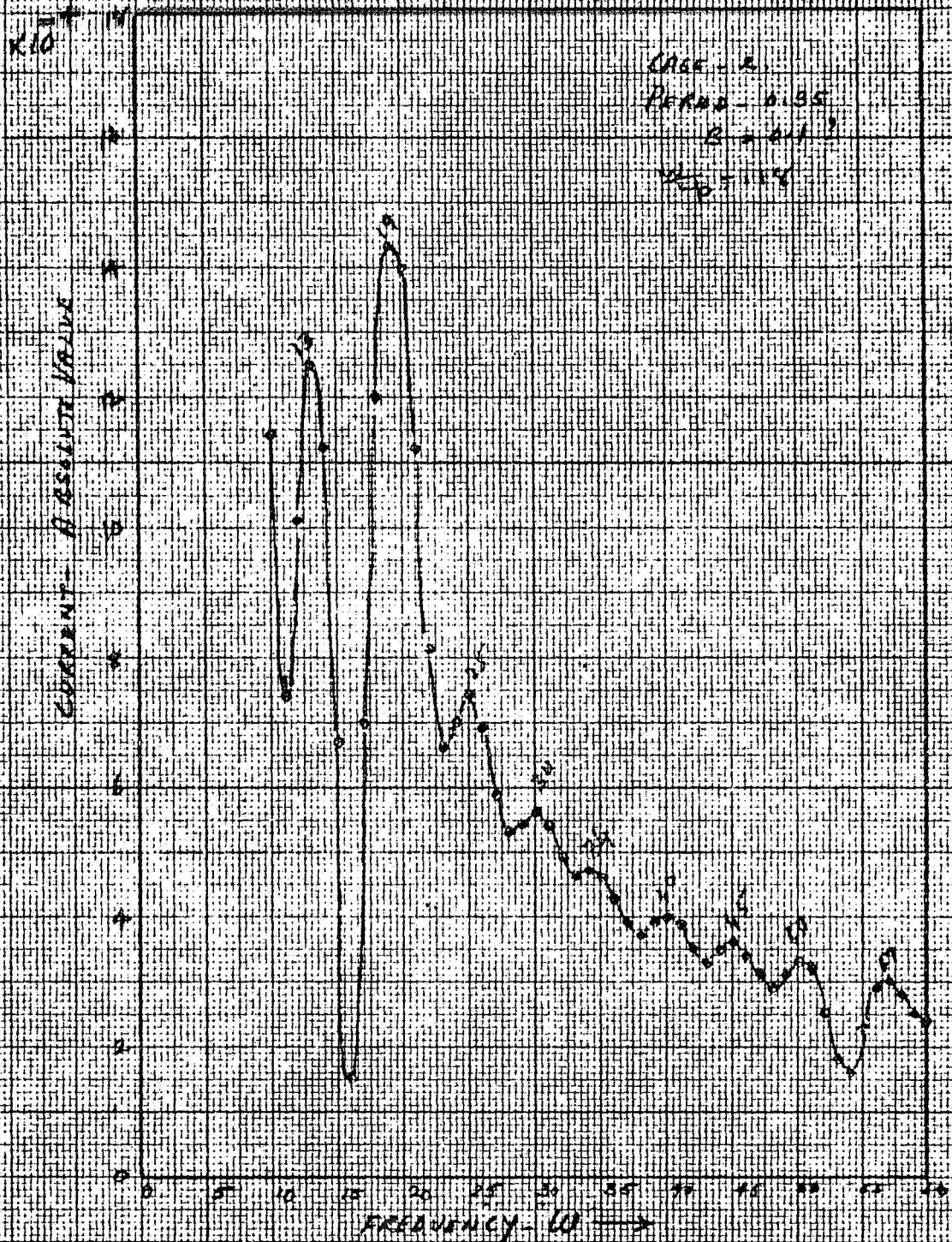


FIGURE - 10

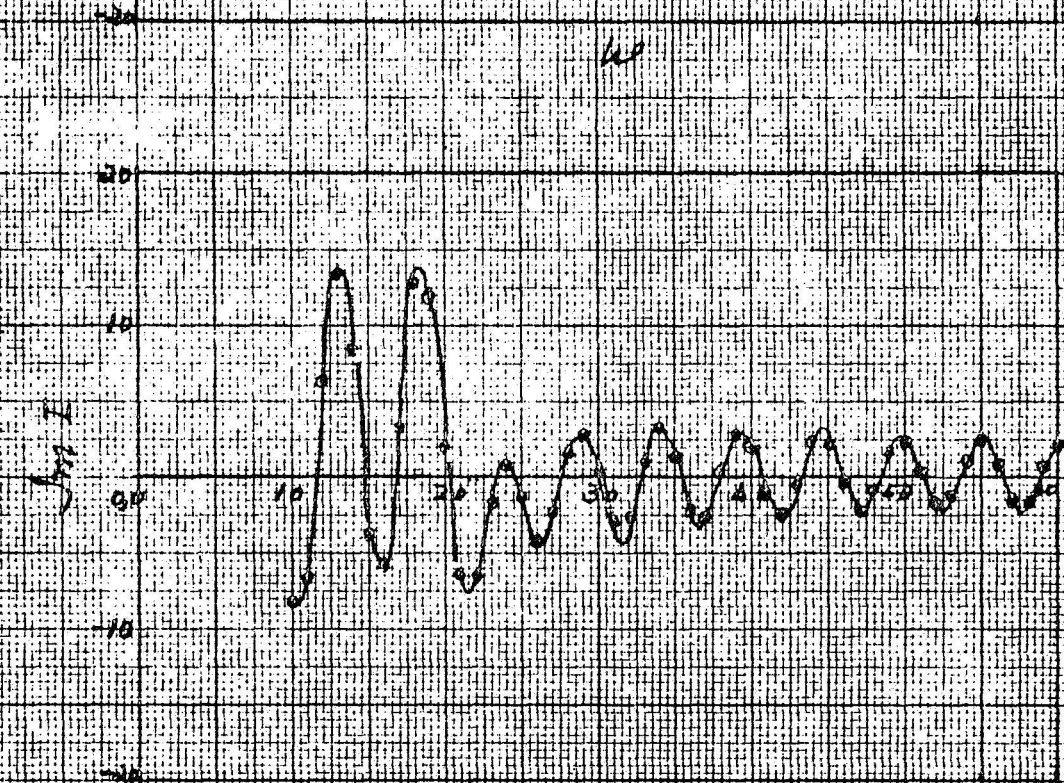
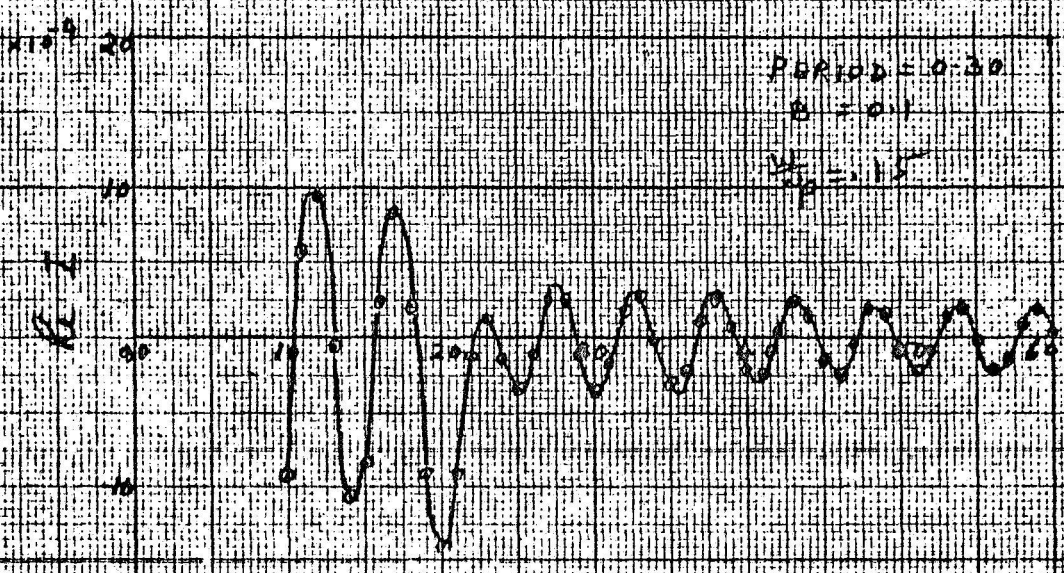


FIGURE 15

W

EUGENE DIETZGEN CO.  
MADE IN U. S. A.

NO. 340R-M DIETZGEN GRAPH PAPER  
MILLIMETER

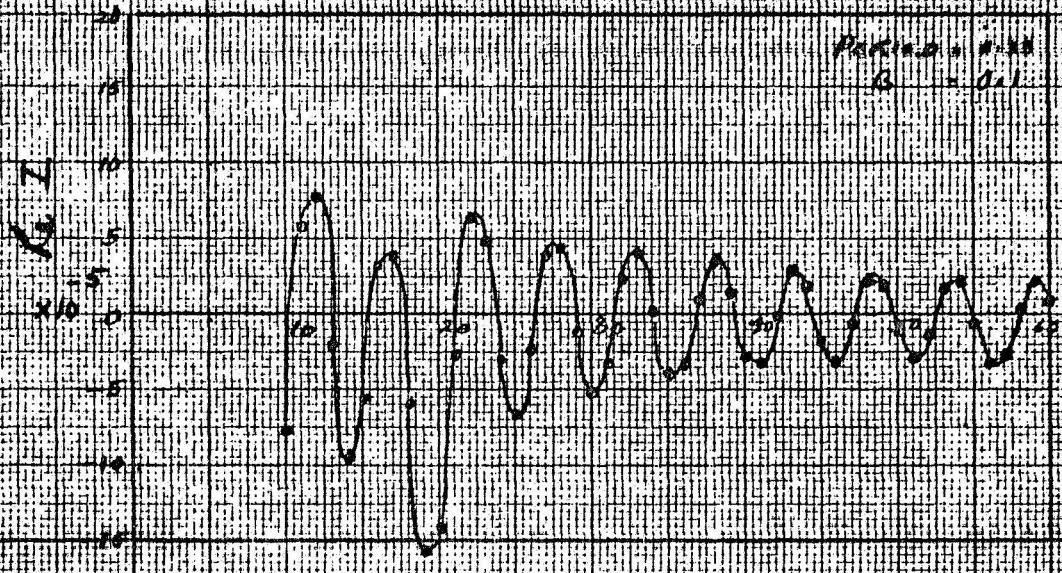


FIGURE-11



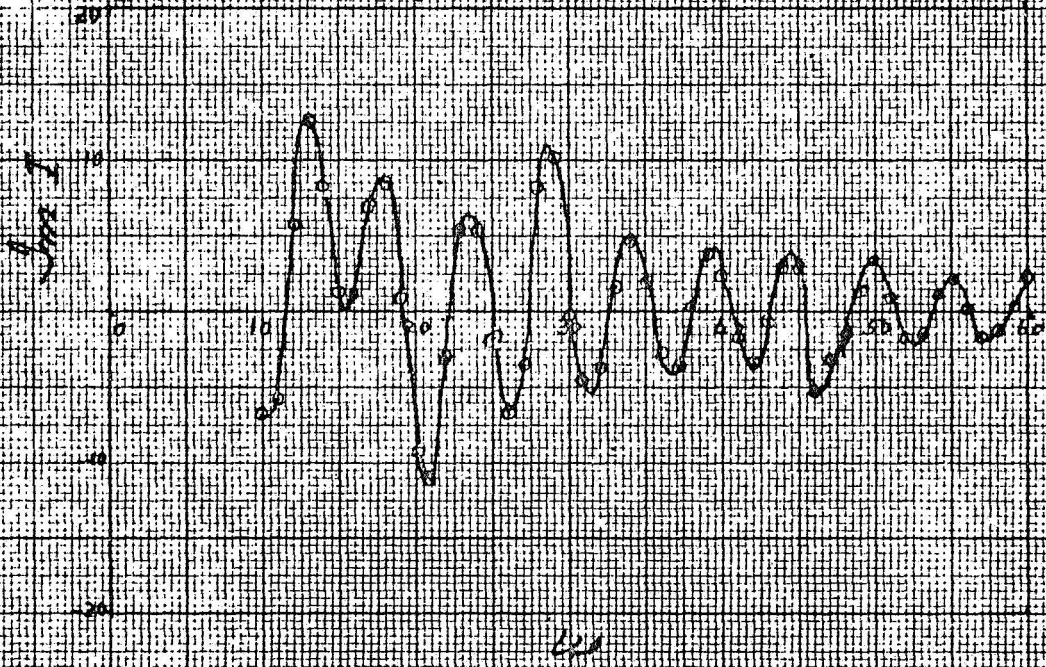
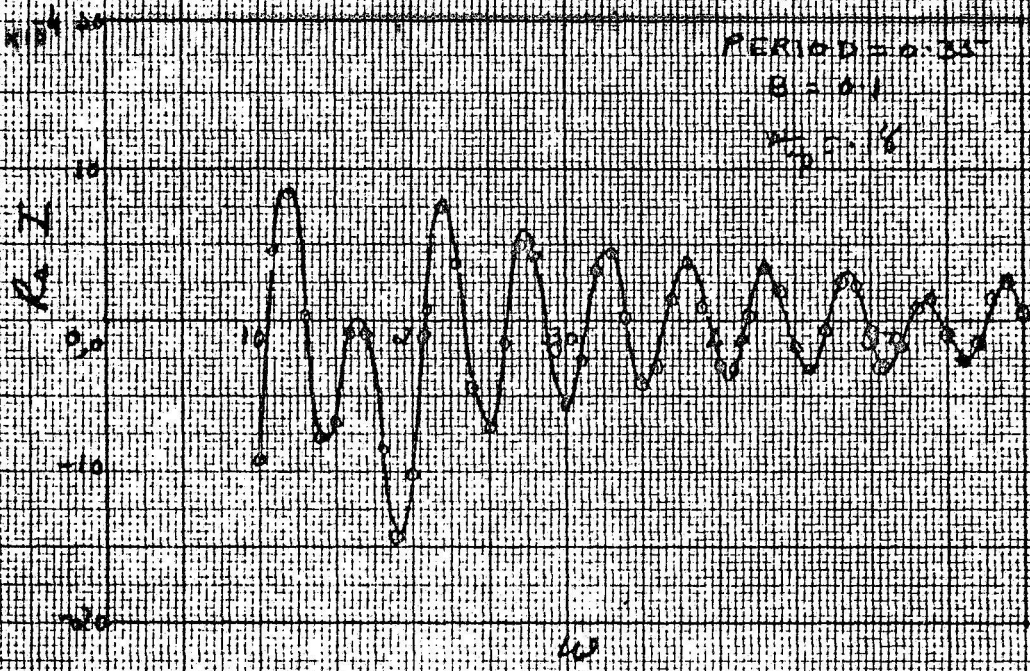


FIGURE-107

## Solutions of the Lenard-Balescu Equation for Drifted Plasmas

by Kurt H. P. H. Sinz and M. Eisner

The effects produced on the plasma distribution by external fields have been investigated in connection with many plasma applications. A starting point which has been usual is the assumption that the principal effects of the external field would be to produce drifted distributions. Thus, if one had initially Maxwellian distributors the effect of the field would be to produce Maxwellian distributions which were drifted in the field direction. Using these distributions one could calculate transport properties. The time development of the distributions is calculated in turn from a kinetic equation with an appropriate collision term. The Lenard-Balescu equation includes a collision term which can be thought of as a collision between dressed particles and therefore includes the effects of wave particle interactions. Since plasma waves may be generated in streaming plasmas the Lenard-Balescu equation would seem to be quite appropriate. In this investigation numerical integration of the kinetic equation is undertaken for a one dimensional drifted plasma with the aim of examining the validity of the drifted distribution assumption and the effects of the wave particle interactions on the time development of the distribution function.

## METHOD OF SOLUTION

The Lenard-Balescu equation given in II-36 is a system of simultaneous, nonlinear, transcendental, integro partial differential equations. For convenience we restate the equations in more explicit form:

$$\frac{\partial f_+}{\partial t} + \frac{m}{M} \frac{E_0}{\lambda_D n_0} \frac{\partial f_+}{\partial v} = - \frac{m}{M 2\pi \lambda_D n_0} \frac{\partial G(v)}{\partial v}$$

and

III - 1

$$\frac{\partial f_-}{\partial t} - \frac{E_0}{\lambda_D n_0} \frac{\partial f_-}{\partial v} = \frac{1}{2\pi \lambda_D n_0} \frac{\partial G(v)}{\partial v}$$

with

$$G(v) = \tan^{-1} \left[ \frac{\pi \frac{\partial}{\partial v} (f_- + \frac{m}{M} f_+)}{P \int_{-\infty}^{\infty} \frac{\partial}{\partial v} (f_- + \frac{m}{M} f_+)} \frac{f_+ \frac{\partial f_-}{\partial v} - \frac{m}{M} f_- \frac{\partial f_+}{\partial v}}{\frac{\partial}{\partial v} (f_- + \frac{m}{M} f_+)} \right]$$

where  $m$  and  $M$  are the electron and ion masses respectively and  $\lambda_D n_0$  is the number of particles of either species per electron Debye length. These equations give the ensemble average single particle distribution functions  $f_+$  and  $f_-$  when an external electric field is included. We shall be interested in possible effects that the right hand interaction term in III-1 may have on the distributions

and any consequences that this may have on the drag and the spectrum of waves given by the dispersion relation. Although this problem appears much too complicated to make an analytical solution possible, it, nevertheless, is simple enough to permit an "exact" numerical analysis. Before embarking upon such a course, we shall attempt to make exact simplifications of III-1.

Let us suppose that for a first approximation we assume the right hand "interaction" term to be negligible so that we trivially solve the resulting partial differential equations to find

$$f_+ = f_+(v - bt) \quad \text{and} \quad f_- = f_-(v - ct)$$

with  $b = \frac{m}{M\lambda_0 n_0} E_0$  and  $c = -\frac{E_0}{\lambda_0 n_0}$

These equations, of course, represent drifting solutions that accelerate constantly in the external field but experience no diffusion or any change in "shape". Utilizing III-2 various attempts were made to evaluate at least the coefficient of the arctangent function in III-1 when using drifted Maxwellians and drifted Maxwellians that experienced only a very small drag. Unfortunately all such efforts were pretty much futile.

To check the possibility of such solutions that experience no effect except that they are drifted in the external field, we eliminate  $G(v)$  between the two equations in III-1 which leads to

$$\frac{\partial}{\partial t} \left[ f_- + \frac{M}{m} f_+ \right] = \frac{1}{\lambda_b n_0} E_0 \frac{\partial}{\partial v} [f_- - f_+] \quad \text{III-3}$$

This equation can be integrated over time when assuming solutions of the form III-2, and performing the derivative on the right hand side of III-3 while using the homogeneity of III-2 in  $v$  and  $t$  and then integrating. With integration limits on  $t$  from 0 to  $t$ , the result is

$$\frac{M}{m} f_+(v,t) + f_-(v,t) = \frac{M}{m} f_+(v,0) + f_-(v,0)$$

Multiplying this result by  $v$  and  $v^2$  respectively, then integrating over  $v$  and differentiating with respect to  $t$ , establishes the conservation of momentum and produces the claim of conservation of energy. The latter conclusion is obviously inappropriate in view of the electrical field that is acting upon the system. We thus know that solutions are not merely drifted and we expect the collision term in III-1 to play a significant part when solving for  $f_+$  and  $f_-$ .

Some insight into the behavior of the interaction term in III-1 may be gained by trying simple distributions for which the principal value integral can be evaluated

exactly. To this end, square, triangular and parabolic distributions do not appear to be too useful because of their inherent discontinuities in slope; however, at least for the latter two, much can be done towards evaluating the collision term. Of considerable usefulness were distributions of the type

$$f(v) = A[(v-1)(v+1)]^{2n}, \quad n=1,2,\dots, \quad -1 \leq v \leq 1 \quad \text{III-4}$$

as they match onto the line  $f=0$  smoothly at  $v = \pm 1$  because at these points the zeroth through  $(2n - 1)^{\text{th}}$  derivatives vanish. Functions constructed in this way bear much resemblance to a Gaussian and can be simultaneously normalized and assigned arbitrary temperatures. In the preliminary stages of this work, much use was made of III-4 with  $n=1$ , although this results in a discontinuous second derivative and therefore a discontinuous interaction term in III-1 at the "ends" of the distributions. This problem can be overcome by using  $n=2$  in III-4. The fact that the principal value integral in III-1 can be evaluated exactly for this type of function was helpful in making rough plots in order to get an intuitive understanding of the functional behavior of the interaction term. This same feature was invaluable in making exact checks of numerical methods when developing the computer program that produced the numerical solutions of III-1.

The numerical techniques employed to solve III-1 are rather straight forward. The basic scheme consists of numerically evaluating the derivatives with respect to velocity of the distribution functions whose values at time  $t_n$  are known for all grid points of  $v$ . These derivatives must be stored in an array as they are all needed when evaluating the principal value integral. Once  $G$  as defined in III-1 has been determined, the necessary differentiation can be performed and we are thus able to solve for the time derivative of the distribution functions for all grid points of  $v$  at time  $t_n$ . This derivative is then used to update all values of the distributions to time  $t_{n+1}$  allowing us to repeat the above cycle for the next time step. The reevaluation of the principal value integral at each time step is very costly since the appropriate integration has to be carried out for each  $v$ . (The computer time goes about as the square of the number of grid points.) Some economy is possible, however, by noticing that in regions where one of the distributions and its first derivative vanish (or are negligibly small) the collision term in III-1 can be ignored and the other distribution simply drifts in that region according to III-2. In such a region, no recalculations are necessary except to adjust the grid spacing and to delete and interpolate data points as appropriate. Unfortunately this also complicates

the required bookkeeping because of the odd grid points that are thus introduced.

A special device must be used to perform the principal value integration because of the singularity in the integrand. The contribution to the integral due to the grid point at the singularity and the two points immediately next to it, is determined by fitting a parabola to the numerator of the integrand and substituting the calculated information into an analytic formula as follows.

In general we have for  $x_2 \neq x_1, x_3$

$$\int_{x_1}^{x_3} \frac{f[x_1] + (x-x_1)f[x_1, x_2] + (x-x_1)(x-x_2)f[x_1, x_2, x_3]}{x_2 - x} dx =$$

$$f[x_1]P_1 + f[x_1, x_2]P_2 + f[x_1, x_2, x_3]P_3$$

where

$$f[x_1] = f(x_1)$$

$$f[x_1, x_2] = \frac{f(x_2) - f(x_1)}{x_2 - x_1}$$

$$f[x_1, x_2, x_3] = \frac{f(x_1)}{(x_1 - x_2)(x_1 - x_3)} + \frac{f(x_2)}{(x_2 - x_1)(x_2 - x_3)} + \frac{f(x_3)}{(x_3 - x_1)(x_3 - x_2)}$$



are the divided differences calculated from the ordinates and abscissas of the grid points that have been fitted and where

$$P_1 = P \int_{x_1}^{x_3} \frac{dx}{x_2 - x} = -\ln \left| \frac{x_2 - x_3}{x_2 - x_1} \right|$$

$$P_2 = P \int_{x_1}^{x_3} \frac{(x - x_2) dx}{x_2 - x} = -(x_3 - x_1) - (x_2 - x_2) \ln \left| \frac{x_3 - x_2}{x_2 - x_1} \right|$$

and

$$P_3 = P \int_{x_1}^{x_3} \frac{(x - x_1)(x - x_2)}{x_2 - x} dx = \frac{(x_2 - x_1)^2}{2} - \frac{(x_2 - x_3)^2}{2} + (-x_1 - x_2 + 2x_2)(x_1 - x_3) - (-x_1 + x_2)(-x_2 + x_2) \ln \left| \frac{x_3 - x_2}{x_2 - x_1} \right|$$

The remaining contribution to the integral can now be evaluated in a straight forward manner with the help of Simpson's rule.

For the first iteration, the distribution functions were advanced according to the first two terms in the Taylor expansion

$$f(v_m, t_{n+1}) = f(v_m, t_n) + \Delta t \left. \frac{\partial f(v_m, t)}{\partial t} \right|_{t=t_n} + \dots$$

Thereafter, we employed the slightly more sophisticated Adam's method

$$f(v_m, t_{n+1}) = f(v_m, t_n) + \Delta t \left[ \left. \frac{\partial f(v_m, t)}{\partial t} \right|_{t=t_n} + \frac{1}{2} \left( \left. \frac{\partial f(v_m, t)}{\partial t} \right|_{t=t_n} - \left. \frac{\partial f(v_m, t)}{\partial t} \right|_{t=t_{n-1}} \right) \right]$$

to advance our solutions in time. This method is equivalent to fitting a parabola to two points when one coordinate and both slopes are known and then extrapolating along this parabola.

Throughout this work derivatives were taken according to

$$f'(v_m) = \frac{f(v_{m+1}) - f(v_{m-1})}{2\Delta v}$$

which can be shown to be accurate to third order. In connection with the damping, third derivatives had to be taken but no extraneous noise was noticed in spite of the fact that numerical differentiation is prone to giving erratic

results.

Needless to say, the distributions have to be terminated somewhere. Since the "widths" of  $f_+$  and  $f_-$  are different there will be regions where both functions are non-zero ("overlap") or where only one function is nonzero.

In the overlap, both distributions can be updated according to the prescription of the previous paragraph; but, as can be seen from III-1, outside this region  $\frac{\partial f_{\pm}}{\partial t} = 0$  for the vanishing function so that a special treatment has to be devised to account for this.

For the sake of definiteness, let us say that both to the left and to the right of  $f_+$  there is a section of  $f_-$ . Now a positive field advances this right section of  $f_-$  according to III-2. Rather than numerically solving III-1 with  $G=0$  and thus preserving the grid spacing, it is deemed more accurate to simply narrow the spacing between the cut-off and the first electron grid point outside the overlap. Inevitably this gap will attempt to become negative (the  $f_-$  grid point tries to enter the overlap) in which case the corresponding data is discarded because in the overlap  $f_-$  is already represented. In order to preserve continuity, the interaction term has to become negligible near the cut-off which is indeed the case. Thermalization and drift will meanwhile drive  $f_+$  to the right outside the overlap where, however,

$$\frac{\partial f_i}{\partial x} = 0$$

so that it becomes necessary to extrapolate  $f_+$ . This is done by fitting a parabola to the last three points of the ion distribution after it has been updated in the overlap. Simultaneously the right section of the electron distribution has advanced to within an odd grid spacing of the old cut-off. In order to keep this odd velocity increment outside the overlap (and thus preventing proliferation) it is necessary to interpolate to mesh the grid points of the two distributions in the new area of overlap. It should be noted that outside the overlap, the right section of the electron distribution experiences no change in shape.

The left section of the electron distribution is driven away from the overlap thus generating an ever growing gap which is filled by interpolation. Although the field drifts the ions to the right, allowance is made for thermalization by extrapolating the ion distribution to the left in the same manner as described in the previous paragraph for the right hand side.

For the actual data runs, the initial conditions for the computer program were always Maxwellian distributions for particles with an ion-electron mass ratio of two to one and with the same ratio applying to the electron-ion temperature. The velocity grid spacing was usually .06; the

$$\frac{\partial f_i}{\partial x} = 0$$

so that it becomes necessary to extrapolate  $f_+$ . This is done by fitting a parabola to the last three points of the ion distribution after it has been updated in the overlap. Simultaneously the right section of the electron distribution has advanced to within an odd grid spacing of the old cut-off. In order to keep this odd velocity increment outside the overlap (and thus preventing proliferation) it is necessary to interpolate to mesh the grid points of the two distributions in the new area of overlap. It should be noted that outside the overlap, the right section of the electron distribution experiences no change in shape.

The left section of the electron distribution is driven away from the overlap thus generating an ever growing gap which is filled by interpolation. Although the field drifts the ions to the right, allowance is made for thermalization by extrapolating the ion distribution to the left in the same manner as described in the previous paragraph for the right hand side.

For the actual data runs, the initial conditions for the computer program were always Maxwellian distributions for particles with an ion-electron mass ratio of two to one and with the same ratio applying to the electron-ion temperature. The velocity grid spacing was usually .06; the

latter enabled the program to perform about sixty iterations in fifteen minutes on a Univac 1108. The number of particles per Debye length  $\lambda_D n_0$  in III-1 was always chosen to be ten with external fields of either one or ten.

With time steps of .016 inverse plasma periods and an external field of 1., the calculational stability of the problem was found to be excellent provided the initial conditions were not too asymmetric. Noise as indicated from the area under the distributions was restricted to the seventh and eighth significant figures. Smoothing techniques were found unnecessary and none were used. We should note, however, that time steps only twice as large caused the calculations to go unstable within a few iterations.

The computer program was developed on an IBM 7094, the data was obtained from runs on a Univac 1108 and all curves were plotted by the SC 4020.

## CONCLUSIONS

Generally there is some doubt as to the usefulness of investigations in one dimension because of the absence of lateral effects. However, it is certainly calculationaly advantageous to reduce the dimensionality of a problem because much simpler equations result. In our case we were able to carry out numerically exact solutions of the one-dimensional Lenard-Balescu equation which enabled us to make a very detailed investigation of our results. Due to the accuracy of the calculations (the normalization of the particle distributions varied only in the seventh significant figure), we were able to tax the precision of our solutions enough to find very marked effects on a time scale as short as one plasma period. Following is a brief summary of some of the detailed effects observed.

It was found that drifted Maxwellian distributions that were separated too much in velocity space did not satisfy the Lenard-Balescu equation due to a discontinuity in the collision current that arises. This discontinuity was caused by the fact that when the representative point associated with the arctangent function in equation III-1 was located in the third quadrant, the passing of the slope function, in the same equation, across the velocity axis resulted in an infinite discontinuity in the collision cur-

rent with no compensating change in sign of the arctangent function which simply passed from a value greater than

$-\pi$  to a value less than  $-\pi$ .

If, however, the distributions are driven towards a large separation when starting from isotropy, a situation is encountered where, at least for our low mass ratio, there is an extremely strong local interaction in velocity space between the ions and electrons. How high the mass and temperature ratios can be without destroying this effect is difficult to assess without further investigation.

However, such interactions do distort not only the electron distribution but the ion distribution as well. Since most plasma parameters such as damping depend on the slopes of the distribution functions of particles in a system, and since derivatives emphasize any irregularity of a function, it is clear that the asymptotic ion behavior in a plasma cannot be adequately described by a Maxwellian that is merely displaced. The interaction between two drifted Maxwellians was seen to be locally strong and very asymmetric so that both distributions undergo a change in shape.

Because of the formal similarity between the one-dimensional and the three-dimensional Lenard-Balescu equations, we have to expect a similar region of strong interaction of the distributions when an external field drives them to anisotropy. This particular interaction casts serious doubt



on Pearson's assumption that the ion distribution in his problem is simply a drifted Maxwellian that experiences no change in shape. Furthermore, a strong interaction as reported here would be prone to generate numerical instabilities of which Pearson reports many.

If in the three-dimensional case there also is a region beyond which displaced Maxwellians cannot satisfy the Lenard-Balescu equation, then it is in doubt whether a rigid ion distribution would permit the electron distribution to become distorted enough to prevent the solutions from entering such a forbidden region.

If the first of these phenomena does indeed have an analog in three dimensions, one would then expect a different contribution to the dispersion relation from the ions. Pearson did not find any appreciable change in the damping and the foregoing could conceivably be a contributing reason.

In the present work it was shown that the Lenard-Balescu term in the Fokker-Planck equation does indeed cause drag and diffusion. The drag was found to increase with the separation of the distributions in velocity space. The average deceleration per particle due to drag reached values of up to 13% of the acceleration due to the field when the distribution separation was about 2.5 thermal velocities.

Although the average ion acceleration was found to decrease, it was observed that the high energy tail of the ion distribution is subject to a constant acceleration with no drag. In spite of the fact that this sets the stage for runaway, the ions on the average, experience a drag.

For thermalization a threshold was found beyond which both the electron and the ion distributions were heated. This threshold was found to be associated with the development of a region of positive slope in the arctangent function of equation III-1.

When initial displacements were large enough to cause changes in the arctangent as described in the previous paragraph, very severe distortions in the distribution functions were found. These distortions in turn gave rise to new wavebands in the dispersion relation. One of these bands corresponds to unstable waves, but it appears possible that the longer time scale effects that would occur when the distributions are allowed to proceed from isotropy to the domain under discussion, would distort the distributions sufficiently to either eliminate this unstable band or to cause it to become stable.

In conclusion we see that even a one-dimensional plasma model displays many physically meaningful properties. Although the detailed computer programming is long and tedious, the many results obtained and their precision are very

gratifying and justify further investigations along these lines. Such investigations might, for example, include a study of the effects due to different external fields as well as different mass ratios and initial conditions. Furthermore, it would also appear that one-dimensional applications shall provide an excellent proving ground for higher order kinetic equations.

## Oscillations in Spatially Inhomogeneous Plasmas

J. C. Baker and M. Eisner

The effects of gross spatial inhomogeneity on the growth rate of instabilities has been investigated. The Vlasov equation is solved assuming a gaussian distribution for the initial density. The distribution function is expanded in a series of Hermite polynomials for both the spatial and velocity dependence. The series are truncated and the set of coupled equations for the time dependent series coefficients are solved numerically. The electric field generated in the plasma is analyzed to obtain the frequency spectrum for several initial conditions on the velocity. The plasma is started from a drifted state with ions and electrons counterstreaming. The directed plasma motion is rapidly dissipated in a turbulent fashion and the energy contained in long wavelength modes is rapidly transferred to shorter modes. The rate of transfer appears to be sufficiently rapid to prevent the growth of instabilities. These results suggest that the stability conditions can be profoundly affected by inhomogeneities.